Signal Processing 94 (2014) 74–80

Contents lists available at SciVerse ScienceDirect

Signal Processing

journal homepage: www.elsevier.com/locate/sigpro

Computationally efficient ESPRIT algorithm for direction-of-arrival estimation based on Nyström method ☆

Cheng Qian [a], Lei Huang [a,*], H.C. So [b]

[a] Department of Electronic and Information Engineering, Shenzhen Graduate School, Harbin Institute of Technology, Shenzhen, China
[b] Department of Electronic Engineering, City University of Hong Kong, Hong Kong

ARTICLE INFO

Article history:
Received 28 December 2012
Received in revised form
12 April 2013
Accepted 8 May 2013
Available online 14 June 2013

Keywords:
Direction-of-arrival
Signal subspace
Eigenvalue decomposition
ESPRIT

ABSTRACT

A low-complexity ESPRIT algorithm for direction-of-arrival (DOA) estimation is devised in this work. Unlike the conventional subspace based methods, the proposed scheme only needs to calculate two sub-matrices of the sample covariance matrix, that is, $\mathbf{R}_{11}\in\mathbb{C}^{K\times K}$ and $\mathbf{R}_{21}\in\mathbb{C}^{(M-K)\times K}$, avoiding its complete computation. Here, M is the number of sensors of the array, K satisfies $P\leq K\leq\min(M,N)$ with P being the number of source signals and N being the number of snapshots. Meanwhile, a Nyström-based approach is utilized to correctly compute the signal subspace which only requires $\mathcal{O}(MK^2)$ flops. Thus, the proposed method has the advantage of computational attractiveness, particularly when $K\ll M$. Furthermore, we derive the asymptotic variances of the estimated DOAs. Numerical results are included to demonstrate the effectiveness of the developed DOA estimator.

1. Introduction

Subspace-based methods for direction-of-arrival (DOA) estimation, such as MUSIC [1] and ESPRIT [2], are a compromise between accuracy and complexity. However, for a large array and/or large samples, they are also computationally intensive as they involve the calculation of sample covariance matrix (SCM) and its eigenvalue decomposition (EVD) to find the signal or noise subspace.

To reduce the computational cost in the conventional subspace-based algorithms, various alternatives have been proposed in the literature. Marcos et al. [3] have proposed to find the noise subspace by using propagator method (PM) without any eigendecomposition, and then employed the MUSIC method for DOA estimation. However, it essentially relies on the SCM which turns out to be computationally demanding, especially when the numbers of array elements and snapshots are large. Xin et al. [4] have suggested a low-complexity subspace-based method which divides a full uniform linear array (ULA) into overlapping forward and backward subarrays and obtained the noise subspace through a linear operation of the combined Hankel covariance matrix. However, these schemes usually provide a poor estimation performance when the number of snapshots is less than the number of sensors.

In this paper, a low-complexity method is devised for DOA estimation. Unlike the conventional DOA estimators, the proposed method only needs to calculate two sub-matrices of the SCM. In particular, we employ an approach that is based on the Nyström method to correctly find the signal subspace, avoiding the direct computation of SCM and its EVD. The Nyström method has been widely used in speeding up algorithms [5,6]. It is first exploited by Williams and Seeger [7] for sparsifying kernel matrices through approximating their entries. Recently, it has been developed for spectral methods such as grouping problem

☆ The work described in this paper was in part supported by the NSFC/RGC Joint Research Scheme sponsored by the Research Grants Council of the Hong Kong and the National Natural Science Foundation of China (Project nos. N-CityU 104/11, 61110229/61161160564), by the National Natural Science under Grants 61222106 and 61171187 and by the Shenzhen Kongqie talent program under Grant YFZZ20111013.

* Corresponding author. Tel.: +86 755 86011571.
E-mail addresses: alextoqc@gmail.com (C. Qian), lhuang8sasp@hotmail.com, lhuang@hitsz.edu.cn (L. Huang), hcso@ee.cityu.edu.hk (H.C. So).

0165-1684/$ - see front matter © 2013 Elsevier B.V. All rights reserved.
http://dx.doi.org/10.1016/j.sigpro.2013.05.007

[8] and normalized cut [9]. By using the Nyström method, we are able to derive a new ESPRIT algorithm which provides the comparable estimation performance with the classical ESPRIT method but requires much less computational cost than the latter, particularly in the large array scenario. It is worth mentioning that we have recently developed its preliminary version in [10] but the expression of the signal subspace component is tedious and it lacks theoretical analysis. Here we also analyze the asymptotic performance of the proposed ESPRIT method in terms of mean square error (MSE). The simulation results are in line with the theoretical analysis.

2. Problem formulation

Consider a ULA with M isotropic sensors. There are P ($P<M$) uncorrelated narrowband source signals impinging on the array from directions $\{\theta_1,\ldots,\theta_P\}$ in the far field. The $M\times 1$ array observation vector is modeled as

$$\mathbf{x}(t)=\mathbf{A}\mathbf{s}(t)+\mathbf{n}(t),\quad t=1,\ldots,N. \tag{1}$$

Here, $\mathbf{A}=[\mathbf{a}(\theta_1),\ldots,\mathbf{a}(\theta_P)]$ is the steering matrix, $\mathbf{s}(t)=[s_1(t),\ldots,s_P(t)]^{\mathrm{T}}$ is the source signal vector, N is the number of available snapshots and the steering vector due to the pth source can be expressed as

$$\mathbf{a}(\theta_p)=[1,e^{j2\pi\sin\theta_p d/\lambda},\ldots,e^{j2\pi(M-1)\sin\theta_p d/\lambda}]^{\mathrm{T}} \tag{2}$$

where $(\cdot)^{\mathrm{T}}$ is the transpose, λ is the carrier wavelength and $d=\lambda/2$ is the interelement spacing. It is assumed that the noise $\mathbf{n}(t)$ is a white Gaussian process with mean zero and covariance $\sigma_n^2\mathbf{I}_M$, where $\mathbf{I}_M$ is the $M\times M$ identity matrix. Moreover, the noise is uncorrelated with the signal $\mathbf{s}(t)$. The covariance matrix of $\mathbf{x}(t)$ is

$$\mathbf{R}=\mathbb{E}[\mathbf{x}(t)\mathbf{x}(t)^{\mathrm{H}}]=\mathbf{A}\mathbf{R}_{\mathbf{s}}\mathbf{A}^{\mathrm{H}}+\sigma_n^2\mathbf{I}_M \tag{3}$$

where $\mathbf{R}_{\mathbf{s}}=\mathbb{E}[\mathbf{s}(t)\mathbf{s}(t)^{\mathrm{H}}]$, $\mathbb{E}[\cdot]$ stands for the mathematical expectation and $(\cdot)^{\mathrm{H}}$ represents the conjugate transpose.

3. ESPRIT algorithm based on Nyström method

3.1. Signal subspace estimation

To exploit the Nyström method for DOA estimation, we decompose the sample data matrix $\mathbf{X}=[\mathbf{x}_1,\ldots,\mathbf{x}_N]$ as

$$\mathbf{X}=\begin{bmatrix}\mathbf{X}_1\\ \mathbf{X}_2\end{bmatrix} \tag{4}$$

where $\mathbf{X}_1\in\mathbb{C}^{K\times N}$ and $\mathbf{X}_2\in\mathbb{C}^{(M-K)\times N}$ are the data submatrices received by the first K sensors and the remaining $(M-K)$ sensors, respectively. Here, K is a user-defined parameter satisfying $K\in\{1,\ldots,M\}$. Let

$$\mathbf{R}_{11}\triangleq\mathbb{E}[\mathbf{X}_1\mathbf{X}_1^{\mathrm{H}}]=\mathbf{A}_1\mathbf{R}_{\mathbf{s}}\mathbf{A}_1^{\mathrm{H}}+\sigma_{\mathbf{n}}^2\mathbf{I}_K \tag{5}$$

$$\mathbf{R}_{21}\triangleq\mathbb{E}[\mathbf{X}_2\mathbf{X}_1^{\mathrm{H}}]=\mathbf{A}_2\mathbf{R}_{\mathbf{s}}\mathbf{A}_1^{\mathrm{H}} \tag{6}$$

where $\mathbf{A}_1=\mathbf{A}(1:K,:)$ represents the first K row vectors of $\mathbf{A}$ and $\mathbf{A}_2=\mathbf{A}(K+1:M,:)$ represents the remaining $(M-K)$ row vectors of $\mathbf{A}$. In order to proceed, we must insure that $\mathbf{R}_{11}$ is of full-rank. Therefore, K should not be less than P but not larger than $\min(M,N)$, i.e., $\{K|P\le K\le\min(M,N)\}$. In general, when M becomes large, K is not needed to increase substantially with M. For example, when M increases from 15 to 30, we choose a relatively small K, such as $K=12$, is enough to ensure accurate DOA estimation and reduce the computational complexity at the same time.

Let $\mathbf{U}_{11}\mathbf{\Lambda}_{11}\mathbf{U}_{11}^{\mathrm{H}}$ be the EVD of $\mathbf{R}_{11}$, where $\mathbf{U}_{11}\in\mathbb{C}^{K\times K}$ is the eigenvector matrix and $\mathbf{\Lambda}_{11}\in\mathbb{C}^{K\times K}$ is the corresponding diagonal matrix with eigenvalues in descending order. Setting $\mathbf{U}_{21}\triangleq\mathbf{R}_{21}\mathbf{U}_{11}\mathbf{\Lambda}_{11}^{-1}$, we form a new matrix as

$$\breve{\mathbf{U}}\triangleq\begin{bmatrix}\mathbf{U}_{11}\\ \mathbf{U}_{21}\end{bmatrix} \tag{7}$$

We would like to form the signal subspace without the computation of SCM and its EVD. With the results in [8], we have the following proposition.

Proposition 1. *Let* $\mathbf{G}=\breve{\mathbf{U}}\mathbf{\Lambda}_{11}^{1/2}$ *and* $\mathbf{U}_{\mathbf{G}}\mathbf{\Lambda}_{\mathbf{G}}\mathbf{U}_{\mathbf{G}}^{\mathrm{H}}$ *be the EVD of* $\mathbf{G}^{\mathrm{H}}\mathbf{G}$, *where* $\mathbf{\Lambda}_{\mathbf{G}}=\mathrm{diag}[\lambda_{G1},\ldots,\lambda_{GK}]$ *is the eigenvalue matrix with* $\lambda_{G1}\ge\cdots\ge\lambda_{GK}$ *and* $\mathbf{U}_{\mathbf{G}}=[\mathbf{u}_{G1},\ldots,\mathbf{u}_{GK}]$ *is the corresponding eigenvector matrix with* $\mathbf{u}_{Gi}$ $(i=1,\ldots,K)$ *being the ith eigenvector. Then the signal subspace is formed by the first P column vectors of* $\mathbf{\Pi}$, *i.e.*,

$$span\{\tilde{\mathbf{U}}_{\mathbf{s}}\}=span\{\mathbf{A}\} \tag{8}$$

where $\tilde{\mathbf{U}}_{\mathbf{s}}\triangleq\mathbf{\Pi}(:,1:P)$ *and* $\mathbf{\Pi}=\mathbf{G}\mathbf{U}_{\mathbf{G}}$.

Proof. The proof is provided in Appendix A.

3.2. DOA estimation

Having attained the signal subspace $\tilde{\mathbf{U}}_{\mathbf{s}}$, we employ the ESPRIT method for DOA estimation. To this end, we decompose the ULA into two subarrays as illustrated in Fig. 1. Let $\mathbf{J}_1=[\mathbf{I}_m,\mathbf{0}_{m\times(M-m)}]$ and $\mathbf{J}_2=[\mathbf{0}_{m\times(M-m)},\mathbf{I}_m]$ be the selection matrices for the two subarrays, where $\mathbf{0}_{m\times(M-m)}$ represents the $m\times(M-m)$ zero matrix and m is the size of subarrays. The displacement between these subarrays are assumed to be $\Delta=(M-m)d$. Then the two identical subarrays in the ULA are described as

$$\mathbf{J}\mathbf{A}=\begin{bmatrix}\mathbf{A}_{\mathrm{s}1}\\ \mathbf{A}_{\mathrm{s}1}\mathbf{\Phi}\end{bmatrix} \tag{9}$$

where

$$\mathbf{J}=\begin{bmatrix}\mathbf{J}_1\\ \mathbf{J}_2\end{bmatrix} \tag{10}$$

$$\mathbf{\Phi}=\mathrm{diag}[e^{j2\pi\ \sin\ \theta_1|\Delta|/\lambda},\ldots,e^{j2\pi\ \sin\ \theta_P|\Delta|/\lambda}]. \tag{11}$$

and $\mathbf{A}_{\mathrm{s}1}=\mathbf{J}_1\mathbf{A}$ is the array manifold of the first subarray.

Since $\tilde{\mathbf{U}}_{\mathbf{s}}$ spans the same range space of $\mathbf{A}$, there exists a nonsingular matrix $\mathbf{T}\in\mathbb{C}^{P\times P}$ such that

$$\mathbf{J}\tilde{\mathbf{U}}_{\mathbf{s}}=\mathbf{J}\mathbf{A}\mathbf{T}. \tag{12}$$

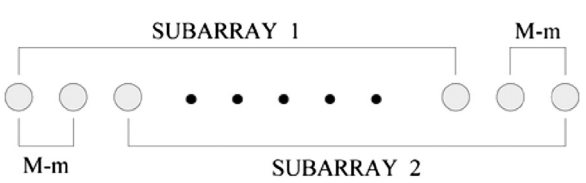

Fig. 1. Subarrays in a ULA. The subarray separation is $(M-m)d$.

Eq. (12) can be rewritten as

$$\begin{bmatrix}\mathbf{J}_1\tilde{\mathbf{U}}_{\mathbf{s}}\\ \mathbf{J}_2\tilde{\mathbf{U}}_{\mathbf{s}}\end{bmatrix}=\begin{bmatrix}\mathbf{U}_{s1}\\ \mathbf{U}_{s2}\end{bmatrix}=\begin{bmatrix}\mathbf{A}_{s1}\mathbf{T}\\ \mathbf{A}_{s1}\boldsymbol{\Phi}\mathbf{T}\end{bmatrix} \tag{13}$$

where $\mathbf{U}_{s1}=\mathbf{J}_1\tilde{\mathbf{U}}_{\mathbf{s}}$ and $\mathbf{U}_{s2}=\mathbf{J}_2\tilde{\mathbf{U}}_{\mathbf{s}}$. From (13), we easily obtain

$$\mathrm{span}(\mathbf{U}_{s1})=\mathrm{span}(\mathbf{U}_{s2})=\mathrm{span}(\mathbf{A}_{s1}). \tag{14}$$

That is, $\mathbf{U}_{s1}$ and $\mathbf{U}_{s2}$ span the same subspace. It follows from (13) that

$$\mathbf{U}_{s2}=\mathbf{U}_{s1}\mathbf{T}^{-1}\boldsymbol{\Phi}\mathbf{T}=\mathbf{U}_{s1}\boldsymbol{\Psi} \tag{15}$$

where $\boldsymbol{\Psi}=\mathbf{T}^{-1}\boldsymbol{\Phi}\mathbf{T}$. Notice that $\boldsymbol{\Phi}$ and $\boldsymbol{\Psi}$ are related by a similarity transformation, and thus have the same eigenvalues. Solving (15) in least-squares sense yields

$$\boldsymbol{\Psi}=\mathbf{U}_{s1}^{\dagger}\mathbf{U}_{s2} \tag{16}$$

where $(\cdot)^{\dagger}$ represents the pseudo-inverse. Performing eigendecomposition to $\boldsymbol{\Psi}$ results in

$$\boldsymbol{\Psi}=\sum_{i=1}^{P}\psi_i\mathbf{e}_i\mathbf{e}_i^{\mathrm{H}} \tag{17}$$

where ψ_i and $\mathbf{e}_i$ are the eigenvalues and eigenvectors of $\boldsymbol{\Psi}$, respectively. As $\boldsymbol{\Psi}$ and $\boldsymbol{\Phi}$ share the same eigenvalues, it follows from (11) that the DOA parameters are estimated as

$$\hat{\theta}_i=\sin^{-1}\left(\frac{\lambda\cdot\angle(\psi_i)}{2\pi|\Delta|}\right),\quad i=1,\ldots,P \tag{18}$$

where $\angle(\psi_i)$ represents the phase angle of the complex number ψ_i. The proposed method for DOA estimation is summarized in Table 1.

3.3. Performance analysis

The asymptotic performance of the ESPRIT has been widely studied in the literature, e.g., Rao and Hari [11] and Li et al. [12,13]. It should be noted that the proposed ESPRIT method is based on the Nyström-based covariance estimator (NCE) [5] and the NCE covariance matrix given in (B.3) has different statistical properties from the SCM. Consequently, the performance of the proposed ESPRIT algorithm differs from that of its counterpart.

Proposition 2. *The asymptotic variance of the proposed version of the ESPRIT method is given as*

$$\mathrm{Var}(\delta\theta_i)=\frac{\nu_i^2}{2}\,\mathrm{Var}(\delta\breve{\psi}_i), \tag{19}$$

where

$$\nu_i=\frac{\lambda}{2\pi\Delta\,\cos\,\theta_i}$$

$$\mathrm{Var}(\delta\psi_i)=\mathbf{W}_i\left(\sum_{j=1}^{P}|x_{ij}|^2\frac{\lambda_j}{N}\sum_{\substack{k=1\\k\neq j}}^{K}\frac{\lambda_k}{(\lambda_j-\lambda_k)^2}\mathbf{u}_k\mathbf{u}_k^{\mathrm{H}}\right)\mathbf{W}_i^{\mathrm{H}}$$

$$\mathbf{W}_i=\mathbf{q}_i\mathbf{U}_{s1}^{\dagger}(\mathbf{J}_1-\psi_i^{*}\mathbf{J}_2). \tag{20}$$

Proof. The proof is provided in Appendix B.

3.4. Computational complexity

The proposed ESPRIT method does not require the formation of the whole SCM. Instead, it only needs to compute $\mathbf{R}_{11}$ and $\mathbf{R}_{12}$ which require $\mathcal{O}(NK^2)$ and $\mathcal{O}(MNK-NK^2)$ flops, respectively. Here, flops stands for complex-valued floating point operations. Meanwhile, we use the Nyström-based approach that just needs $\mathcal{O}(MK^2)$ flops to construct the signal subspace. Therefore, the proposed method requires $\mathcal{O}(MNK+MK^2)$ flops. However, the classical ESPRIT algorithm needs $\mathcal{O}(M^2N+M^3)$ flops, which is much larger than $\mathcal{O}(MNK+MK^2)$ flops provided that $K\ll\min(M,N)$.

4. Simulation results

We compare the proposed ESPRIT method with the classical ESPRIT and unitary ESPRIT methods in terms of root mean square error (RMSE). Meanwhile, the theoretical MSEs of the proposed and classical ESPRIT algorithms are plotted as well. In this simulation, two narrowband Gaussian signals with zero-mean and variance σ^2 are assumed to impinge upon a ULA from directions $\theta_1=1^{\circ}$ and $\theta_2=8^{\circ}$. The noise is the zero-mean white Gaussian process. The signal-to-noise ratio (SNR) is defined as the ratio of the power of the source signals to that of the additive noise. The displacement between two subarrays is assumed to be $d=\lambda/2$. Monte Carlo simulation is carried out to evaluate the RMSE and all the numerical results are averaged from

Table 1
Proposed algorithm.

Step 1	Decompose $\mathbf{X}$ into two sub-matrices $\mathbf{X}_1$ and $\mathbf{X}_2$ as (4). Then calculate the estimates of $\mathbf{R}_{11}$ and $\mathbf{R}_{21}$ from N snapshots, i.e., $\hat{\mathbf{R}}_{11}=(1/N)\mathbf{X}_1\mathbf{X}_1^{\mathrm{H}}$ and $\hat{\mathbf{R}}_{21}=(1/N)\mathbf{X}_2\mathbf{X}_1^{\mathrm{H}}$.
Step 2	Perform the EVD of $\hat{\mathbf{R}}_{11}$ and set $\hat{\mathbf{U}}_{21}\triangleq\hat{\mathbf{R}}_{21}\hat{\mathbf{U}}_{11}\hat{\boldsymbol{\Lambda}}_{11}^{-1}$, $\hat{\mathbf{U}}\triangleq[\hat{\mathbf{U}}_{11}^{\mathrm{T}}\ \hat{\mathbf{U}}_{21}^{\mathrm{T}}]^{\mathrm{T}}$.
Step 3	Construct the matrix $\hat{\mathbf{G}}=\hat{\mathbf{U}}\hat{\boldsymbol{\Lambda}}_{11}$ and perform the EVD of $\hat{\mathbf{G}}^{\mathrm{H}}\hat{G}$, i.e., $\hat{\mathbf{G}}^{\mathrm{H}}\hat{\mathbf{G}}=\hat{\mathbf{U}}_{\mathbf{G}}\hat{\boldsymbol{\Lambda}}_{\mathbf{G}}\hat{\mathbf{U}}_{\mathbf{G}}^{\mathrm{H}}$. Let $\hat{\boldsymbol{\Pi}}=\hat{\mathbf{G}}\hat{\mathbf{U}}_{\mathbf{G}}$, then the signal subspace is formed by the first P column vectors of $\hat{\boldsymbol{\Pi}}$, that is, $\hat{\mathbf{U}}_s=\hat{\boldsymbol{\Pi}}(:,1:P)$.
Step 4	Define two selected matrices $\mathbf{J}_1=[\mathbf{I}_m,\mathbf{0}_{m\times(M-m)}]$ and $\mathbf{J}_2=[\mathbf{0}_{m\times(M-m)},\mathbf{I}_m]$. The signal subspace formed by the two subarrays can be expressed as $\hat{\mathbf{U}}_{s1}=\mathbf{J}_1\hat{\mathbf{U}}_{\mathbf{s}}$ and $\hat{\mathbf{U}}_{s2}=\mathbf{J}_2\hat{\mathbf{U}}_{\mathbf{s}}$, respectively. Utilize least squares to obtain $\hat{\boldsymbol{\Psi}}=\hat{\mathbf{U}}_{s1}^{\dagger}\hat{\mathbf{U}}_{s2}$. Perform the EVD of $\hat{\boldsymbol{\Psi}}$ to obtain $\hat{\boldsymbol{\Psi}}=\sum_{i=1}^{P}\hat{\psi}_i\hat{\mathbf{e}}_i\hat{\mathbf{e}}_i^{\mathrm{H}}$.
Step 5	The DOA parameters are estimated as $\hat{\theta}_i=\sin^{-1}\left(\frac{\lambda\cdot\angle(\hat{\psi}_i)}{2\pi\lvert\Delta\rvert}\right)$.

1000 independent runs. The RMSE is defined as

$$\mathrm{RMSE}=\sqrt{\mathbb{E}\left\{\frac{1}{P}\sum_{i=1}^{P}(\hat{\theta}_i-\theta_i)^2\right\}}. \tag{21}$$

The RMSEs are depicted in Figs. 2 and 3 as a function of SNR for different parameter settings. It can be seen that in the high SNR regime, the proposed ESPRIT algorithm provides similar performance as the classical and unitary ESPRIT methods no matter how small or large the K is. This in turn implies that the proposed ESPRIT method is not very sensitive to the selection of K provided that $K\geq P$. Therefore, when M and N are fixed, we can choose a relatively small K in large SNR scenario to save the computational cost. Figs. 2 and 3 also imply that a relatively larger K can only lead to a bit better performance for the proposed method. Meanwhile, it is indicated in the figures that as M becomes larger, K should be increased accordingly.

We now study the RMSE as a function of the sample size. It is observed from Figs. 4 and 5 that, when $N\leq 40$, the proposed ESPRIT scheme achieves the performance that is almost the same as the classical and unitary ESPRIT methods. When $N>40$ and $K=10$, however, the former is somewhat inferior to the conventional approach. As K becomes larger, say, $K=12$, the proposed ESPRIT method provides comparable performance with the other two ESPRIT algorithms.

The computational times of the three ESPRIT algorithms versus M with $K=5,10,15$ are plotted in Fig. 6. It provides the average CPU time required to compute each ESPRIT algorithm on a personal computer with an Intel i3-2120 3.3 GHz processor. We observe that the proposed ESPRIT algorithm is much computationally simpler than the other two ESPRIT algorithms, particularly when M becomes larger.

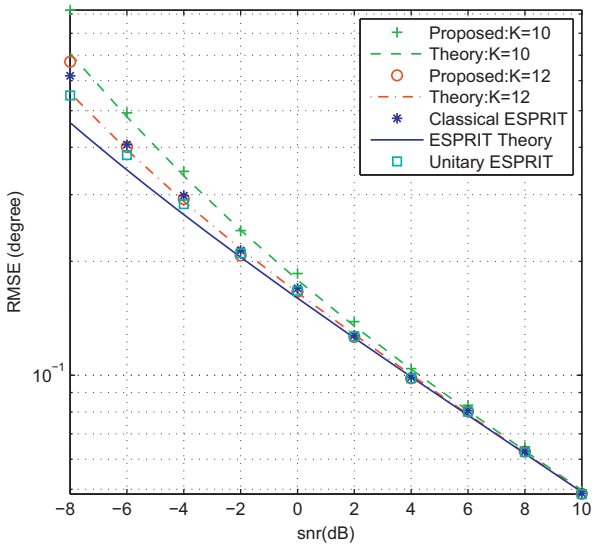

Fig. 2. RMSE angle error performance in small-scale array case ($M=15$, $m=14$, $N=100$, $K=[10;12]$).

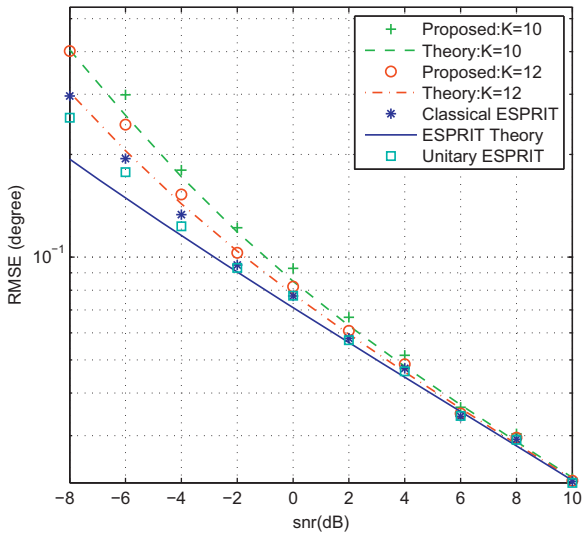

Fig. 3. RMSE angle error performance in large-scale array case ($M=30$, $m=29$, $N=100$, $K=[10;12]$).

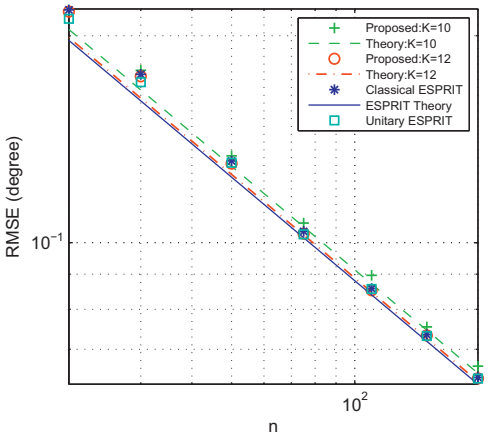

Fig. 4. RMSE angle error performance versus N ($M=15$, $m=14$, $K=[10;12]$, SNR$=5$ dB).

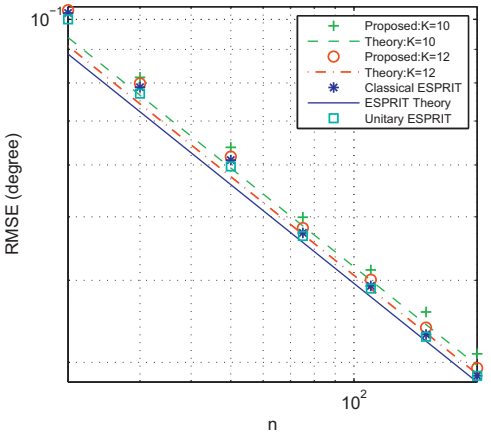

Fig. 5. RMSE angle error performance versus N ($M=30$, $m=29$, $K=[10;12]$, SNR$=5$ dB).

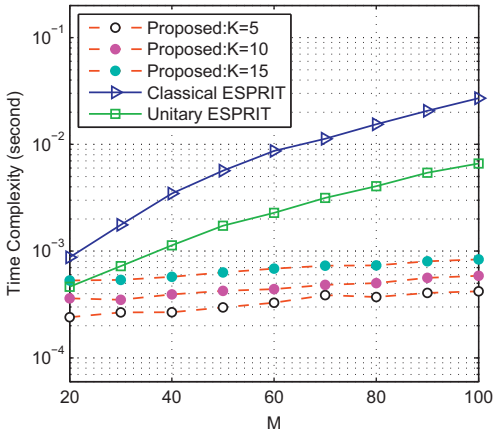

Fig. 6. Computational time versus M ($m=M-1$, $N=100$, $P=2$, $K=[5; 10; 15]$).

5. Conclusion

A low-complexity ESPRIT algorithm has been devised for DOA estimation. In contrast to the existing ESPRIT methods which require $\mathcal{O}(M^2N+M^3)$ flops, the proposed scheme only needs $\mathcal{O}(MNK+MK^2)$ flops, thereby being more computationally efficient, especially for the case of a large array. We also derive the theoretical expression for the asymptotic variances of the DOA estimates. Numerical results demonstrate that our proposal can provide comparable performance with the classical and unitary ESPRIT methods.

Appendix A. Proof of Proposition 1

Let $\mathbf{U_s}$ be the true signal subspace and there exists a full-rank matrix $\mathbf{T}$ such that $\mathbf{U_s}=\mathbf{AT}$. Note that $\mathbf{\Pi}$ can be rewritten as

$$\begin{aligned}\mathbf{\Pi}&=\mathbf{GU_G}\\&=\begin{bmatrix}\mathbf{U}_{11}\\ \mathbf{R}_{21}\mathbf{U}_{11}\mathbf{\Lambda}_{11}^{-1}\end{bmatrix}(\mathbf{\Lambda}_{11}\mathbf{U}_{11}^{\mathrm{H}})\cdot(\mathbf{\Lambda}_{11}\mathbf{U}_{11}^{\mathrm{H}})^{-1}\mathbf{\Lambda}_{11}^{1/2}\mathbf{U_G}\\&=\begin{bmatrix}\mathbf{U}_{11}\mathbf{\Lambda}_{11}\mathbf{U}_{11}^{\mathrm{H}}\\ \mathbf{R}_{21}\end{bmatrix}\mathbf{U}_{11}\mathbf{\Lambda}_{11}^{-1/2}\mathbf{U_G}\\&=\begin{bmatrix}\mathbf{R}_{11}\\ \mathbf{R}_{21}\end{bmatrix}\mathbf{Q}\end{aligned}\tag{A.1}$$

where $\mathbf{Q}=\mathbf{U}_{11}\mathbf{\Lambda}_{11}^{-1/2}\mathbf{U_G}\in\mathbb{C}^{K\times K}$ is a full-rank matrix because $\mathbf{U}_{11}$, $\mathbf{\Lambda}_{11}$ and $\mathbf{U_G}$ are the full-rank matrices. According to (5) and (6), we obtain

$$\begin{aligned}\begin{bmatrix}\mathbf{R}_{11}\\ \mathbf{R}_{21}\end{bmatrix}&=\begin{bmatrix}\mathbf{A}_1\mathbf{R_s}\mathbf{A}_1^{\mathrm{H}}\\ \mathbf{A}_2\mathbf{R_s}\mathbf{A}_1^{\mathrm{H}}\end{bmatrix}+\begin{bmatrix}\sigma_{\mathbf{n}}^2\mathbf{I}_K\\ \mathbf{0}_{(M-K)\times K}\end{bmatrix}\\&=\mathbf{AR_s}\mathbf{A}_1^{\mathrm{H}}+\mathbf{AA}^{\dagger}\begin{bmatrix}\sigma_{\mathbf{n}}^2\mathbf{I}_K\\ \mathbf{0}_{(M-K)\times K}\end{bmatrix}\\&=\mathbf{A}\left(\mathbf{R_s}\mathbf{A}_1^{\mathrm{H}}+(\mathbf{A}^{\mathrm{H}}\mathbf{A})^{-1}\mathbf{A}^{\mathrm{H}}\begin{bmatrix}\sigma_{\mathbf{n}}^2\mathbf{I}_K\\ \mathbf{0}_{(M-K)\times K}\end{bmatrix}\right]\\&=\mathbf{A}(\mathbf{R_s}+\sigma_{\mathbf{n}}^2(\mathbf{A}^{\mathrm{H}}\mathbf{A})^{-1})\mathbf{A}_1^{\mathrm{H}}.\end{aligned}\tag{A.2}$$

Substituting (A.2) into (A.1) yields

$$\begin{aligned}\mathbf{\Pi}&=\mathbf{A}(\mathbf{R_s}+\sigma_{\mathbf{n}}^2(\mathbf{A}^{\mathrm{H}}\mathbf{A})^{-1})\mathbf{A}_1^{\mathrm{H}}\mathbf{Q}\\&=\mathbf{AB}\mathbf{A}_1^{\mathrm{H}}\mathbf{Q}\end{aligned}\tag{A.3}$$

where $\mathbf{B}=\mathbf{R_s}+\sigma_{\mathbf{n}}^2(\mathbf{A}^{\mathrm{H}}\mathbf{A})^{-1}\in\mathbb{C}^{P\times P}$.

Note that

$$\begin{aligned}\mathbf{R_x}&=\mathbf{U_s}\mathbf{\Lambda_s}\mathbf{U_s}^{\mathrm{H}}+\sigma_{\mathbf{n}}^2\mathbf{U_n}\mathbf{U_n}^{\mathrm{H}}\\&=\mathbf{AR_s}\mathbf{A}^{\mathrm{H}}+\sigma_{\mathbf{n}}^2\mathbf{I}_M.\end{aligned}\tag{A.4}$$

Post-multiplying (A.4) with $\mathbf{U_s}$ yields

$$\mathbf{AR_s}\mathbf{A}^{\mathrm{H}}\mathbf{U_s}=\mathbf{U_s}(\mathbf{\Lambda_s}-\sigma_{\mathbf{n}}^2\mathbf{I}_M).\tag{A.5}$$

Since $\mathbf{U_s}\mathbf{U_s}^{\mathrm{H}}=\mathbf{AA}^{\mathrm{H}}\mathbf{A}^{-1}\mathbf{A}^{\mathrm{H}}$, it follows from (A.5) that

$$\begin{aligned}\mathbf{R_s}&=\mathbf{A}^{\dagger}\mathbf{U_s}(\mathbf{\Lambda_s}-\sigma_{\mathbf{n}}^2\mathbf{I}_M)\mathbf{U_s}^{\mathrm{H}}(\mathbf{A}^{\dagger})^{\mathrm{H}}\\&=\mathbf{A}^{\dagger}\mathbf{U_s}\mathbf{\Lambda_s}\mathbf{U_s}^{\mathrm{H}}(\mathbf{A}^{\dagger})^{\mathrm{H}}-\sigma_{\mathbf{n}}^2\mathbf{A}^{\dagger}\mathbf{U_s}\mathbf{U_s}^{\mathrm{H}}(\mathbf{A}^{\dagger})^{\mathrm{H}}\\&=\mathbf{A}^{\dagger}\mathbf{U_s}\mathbf{\Lambda_s}\mathbf{U_s}^{\mathrm{H}}(\mathbf{A}^{\dagger})^{\mathrm{H}}-\sigma_{\mathbf{n}}^2(\mathbf{A}^{\mathrm{H}}\mathbf{A})^{-1}.\end{aligned}\tag{A.6}$$

As a result, recalling that $\mathbf{B}=\mathbf{R_s}+\sigma_{\mathbf{n}}^2(\mathbf{A}^{\mathrm{H}}\mathbf{A})^{-1}$, we get

$$\mathbf{B}=\mathbf{A}^{\dagger}\mathbf{U_s}\mathbf{\Lambda_s}\mathbf{U_s}^{\mathrm{H}}(\mathbf{A}^{\dagger})^{\mathrm{H}}.\tag{A.7}$$

Substituting $\mathbf{U_s}=\mathbf{AT}$ into (A.7), we obtain

$$\mathbf{B}=\mathbf{T}\mathbf{\Lambda_s}\mathbf{T}^{\mathrm{H}}.\tag{A.8}$$

Since $\mathbf{T}$ and $\mathbf{\Lambda_s}$ are full-rank matrices with rank P, we have $\mathrm{rank}(\mathbf{B})=P$. That is, $\mathbf{B}$ is also a full-rank matrix.

Let $\mathbf{H}=\mathbf{B}\mathbf{A}_1^{\mathrm{H}}\mathbf{Q}$, then $\mathbf{\Pi}=\mathbf{AH}$. Due to the Vandermonde structure of $\mathbf{A}_1^{\mathrm{H}}\in\mathbb{C}^{P\times K}$, the first P column vectors in $\mathbf{H}$ are linearly independent. Hence, there must exist a full-rank matrix $\tilde{\mathbf{T}}$ such that

$$\tilde{\mathbf{U}}_{\mathbf{s}}=\mathbf{\Pi}(:,1:P)=\mathbf{A}\tilde{\mathbf{T}}\tag{A.9}$$

where $\tilde{\mathbf{T}}=\mathbf{H}(:,1:P)$. This completes the proof of Proposition 1.

Appendix B. Proof of Proposition 2

Let $\tilde{\mathbf{\Pi}}=\mathbf{\Pi}\mathbf{\Lambda}_{\mathbf{G}}^{-1/2}$. Then, it is easy to verify that

$$\begin{aligned}\tilde{\mathbf{\Pi}}^{\mathrm{H}}\tilde{\mathbf{\Pi}}&=\mathbf{\Lambda}_{\mathbf{G}}^{-1/2}\mathbf{U}_{\mathbf{G}}^{\mathrm{H}}\mathbf{G}^{\mathrm{H}}\cdot\mathbf{GU_G}\mathbf{\Lambda}_{\mathbf{G}}^{-1/2}\\&=\mathbf{\Lambda}_{\mathbf{G}}^{-1/2}\mathbf{U}_{\mathbf{G}}^{\mathrm{H}}\cdot\mathbf{U_G}\mathbf{\Lambda_G}\mathbf{U}_{\mathbf{G}}^{\mathrm{H}}\cdot\mathbf{U_G}\mathbf{\Lambda}_{\mathbf{G}}^{-1/2}\\&=\mathbf{I}_K.\end{aligned}\tag{B.1}$$

Therefore, the column vectors in $\tilde{\mathbf{\Pi}}$ are mutually orthogonal.

Let $\tilde{\mathbf{\Pi}}$ be the eigenvector matrix and $\mathbf{\Lambda_G}$ be the corresponding eigenvalue matrix. Then the EVD formed by $\mathbf{\Lambda_G}$ and $\tilde{\mathbf{\Pi}}$ can be expressed as

$$\begin{aligned}\tilde{\mathbf{\Pi}}\mathbf{\Lambda_G}\tilde{\mathbf{\Pi}}^{\mathrm{H}}&=\mathbf{GU_G}\mathbf{\Lambda}_{\mathbf{G}}^{-1/2}\cdot\mathbf{\Lambda_G}\cdot\mathbf{\Lambda}_{\mathbf{G}}^{-1/2}\mathbf{U}_{\mathbf{G}}^{\mathrm{H}}\mathbf{G}^{\mathrm{H}}=\mathbf{GG}^{\mathbf{H}}\\&=\begin{bmatrix}\mathbf{U}_{11}\\ \mathbf{R}_{21}\mathbf{U}_{11}\mathbf{\Lambda}_{11}^{-1}\end{bmatrix}\mathbf{\Lambda}_{11}^{1/2}\cdot\mathbf{\Lambda}_{11}^{1/2}[\mathbf{U}_{11}^{\mathrm{H}}\ \ \mathbf{\Lambda}_{11}^{-1}\mathbf{U}_{11}^{\mathrm{H}}\mathbf{R}_{21}^{\mathrm{H}}]\\&=\begin{bmatrix}\mathbf{R}_{11} & \mathbf{R}_{21}^{\mathrm{H}}\\ \mathbf{R}_{21} & \mathbf{R}_{21}\mathbf{R}_{11}^{-1}\mathbf{R}_{21}^{\mathrm{H}}\end{bmatrix}.\end{aligned}\tag{B.2}$$

Setting $\mathbf{R}_{12}\triangleq\mathbb{E}\{\mathbf{X}_1\mathbf{X}_2^{\mathrm{H}}\}=\mathbf{R}_{21}^{\mathrm{H}}$, (B.2) can also be written as

$$\mathbf{R}_{\mathrm{NCE}}=\begin{bmatrix}\mathbf{R}_{11} & \mathbf{R}_{12}\\ \mathbf{R}_{21} & \mathbf{R}_{21}\mathbf{R}_{11}^{-1}\mathbf{R}_{12}\end{bmatrix}.\tag{B.3}$$

Here, $\mathbf{R}_{\mathrm{NCE}}$ is the covariance matrix obtained by the Nyström-based covariance estimator [5] which is a fast

low-rank approximation of a large positive semi-definite matrix and can provide comparable performance with the SCM.

The EVD of the NCE covariance matrix is given as

$$\mathbf{R}_{\mathrm{NCE}} = \sum_{i=1}^{M} \lambda_i \mathbf{u}_i \mathbf{u}_i^{\mathrm{H}} \tag{B.4}$$

where $\lambda_1 \geq \cdots \geq \lambda_P \geq \lambda_{P+1} = \cdots = \lambda_K = \sigma_n^2$ are the nonzero eigenvalues and $\mathbf{u}_i, i = 1, \ldots, K$, are the corresponding eigenvectors. Since $\mathrm{rank}(\mathbf{R}_{\mathrm{NCE}}) = \mathrm{rank}(\mathbf{R}_{11}) = K$, we have $\lambda_{K+1} = \cdots = \lambda_M = 0$.

As the quantity of interest is θ_i, we need to find the relationship between the error in θ_i and the error in ψ_i. Noticing that $\psi_i = e^{j2\pi \sin \theta_i \Delta/\lambda}$ and performing first-order Taylor series expansion [13], we have

$$\begin{aligned} \delta\theta_i &\approx \frac{\lambda}{2\pi\Delta \cos \theta_i} \mathrm{Re}\left\{\frac{\delta\psi_i}{j\psi_i}\right\} \\ &= \nu_i \, \mathrm{Im}\{\breve{\delta\psi}_i\} \end{aligned} \tag{B.5}$$

where $\mathrm{Re}\{\cdot\}$ and $\mathrm{Im}\{\cdot\}$ stands for the real and imaginary parts respectively,

$$\breve{\delta\psi}_i = \frac{\delta\psi_i}{\psi_i} \quad \text{and} \quad \nu_i = \frac{\lambda}{2\pi\Delta \cos \theta_i}. \tag{B.6}$$

The error-variance of the estimated DOA is

$$\mathrm{Var}(\delta\theta_i) = \nu_i^2 \, \mathrm{Var}(\mathrm{Im}\{\breve{\delta\psi}_i\}) = \frac{\nu_i^2}{2} \, \mathrm{Var}(\breve{\delta\psi}_i). \tag{B.7}$$

The next step is to find the variance of $\breve{\delta\psi}_i$. In Section 3, we compute the matrix $\boldsymbol{\Psi}$ as

$$\boldsymbol{\Psi} = \mathbf{U}_{s1}^{\dagger} \mathbf{U}_{s2}. \tag{B.8}$$

Let $\mathbf{q}_i$ be the corresponding left eigenvector. It follows from (17) that

$$\boldsymbol{\Psi}\mathbf{e}_i = \psi_i \mathbf{e}_i \tag{B.9}$$

$$\mathbf{q}_i \boldsymbol{\Psi} = \psi_i \mathbf{q}_i. \tag{B.10}$$

Note that, $\mathbf{q}_i$ and $\mathbf{e}_i$ satisfy $\mathbf{q}_i \mathbf{e}_i = 1$ [15]. According to (B.(9) and B.10), we obtain

$$\psi_i = \mathbf{q}_i \boldsymbol{\Psi} \mathbf{e}_i. \tag{B.11}$$

In most of the practical applications, there are lots of factors, such as the noise and finite data, resulting in an error $\delta\boldsymbol{\Psi}$ in the estimation of $\boldsymbol{\Psi}$. Therefore, the error $\delta\psi_i$ in the estimated eigenvalue $\hat{\psi}_i$ is inevitable. Employing first-order approximation, $\delta\psi_i$ can be written as

$$\delta\psi_i \approx \mathbf{q}_i \delta\boldsymbol{\Psi} \mathbf{e}_i. \tag{B.12}$$

It follows from $\mathbf{U}_{s1}\boldsymbol{\Psi} = \mathbf{U}_{s2}$ that

$$(\mathbf{U}_{s1} + \delta\mathbf{U}_{s1})(\boldsymbol{\Psi} + \delta\boldsymbol{\Psi}) = \mathbf{U}_{s2} + \delta\mathbf{U}_{s2} \tag{B.13}$$

Canceling $\mathbf{U}_{s1}\boldsymbol{\Psi}$ and $\mathbf{U}_{s2}$ and then neglecting the second-order term $\delta\mathbf{U}_{s1}\delta\boldsymbol{\Psi}$ yield

$$\mathbf{U}_{s1}\delta\boldsymbol{\Psi} \approx \delta\mathbf{U}_{s2} - \delta\mathbf{U}_{s1}\boldsymbol{\Psi} \tag{B.14}$$

and

$$\delta\boldsymbol{\Psi} \approx \mathbf{U}_{s1}^{\dagger}\delta\mathbf{U}_{s2} - \mathbf{U}_{s1}^{\dagger}\delta\mathbf{U}_{s1}\boldsymbol{\Psi}. \tag{B.15}$$

Since $|\psi_i| = 1$, substituting (B.15) into (B.12) we have

$$\begin{aligned} \delta\psi_i &\approx \mathbf{q}_i \mathbf{U}_{s1}^{\dagger}(\delta\mathbf{U}_{s2} - \delta\mathbf{U}_{s1}\boldsymbol{\Psi})\mathbf{e}_i \\ &= \mathbf{q}_i \mathbf{U}_{s1}^{\dagger}(\delta\mathbf{U}_{s2}\mathbf{e}_i - \psi_i \delta\mathbf{U}_{s1}\mathbf{e}_i) \\ &= -\psi_i \mathbf{q}_i \mathbf{U}_{s1}^{\dagger}(\mathbf{J}_1 - \psi_i^* \mathbf{J}_2)\delta\mathbf{U}_{\mathbf{s}}\mathbf{e}_i \end{aligned} \tag{B.16}$$

where

$$\delta\mathbf{U}_{\mathbf{s}} = \hat{\mathbf{U}}_{\mathbf{s}} - \mathbf{U}_{\mathbf{s}}. \tag{B.17}$$

Premultiplying $1/\psi_i$ on (B.16) yields

$$\breve{\delta\psi}_i = -\mathbf{q}_i \mathbf{U}_{s1}^{\dagger}(\mathbf{J}_1 - \psi_i^* \mathbf{J}_2)\delta\mathbf{U}_{\mathbf{s}}\mathbf{e}_i. \tag{B.18}$$

It follows from (B.18) that the variance of $\breve{\delta\psi}_i$ is

$$\begin{aligned} \mathrm{Var}(\breve{\delta\psi}_i) &= \mathbf{q}_i \mathbf{U}_{s1}^{\dagger}(\mathbf{J}_1 - \psi_i^* \mathbf{J}_2) \cdot \mathrm{Var}(\delta\mathbf{U}_{\mathbf{s}}\mathbf{e}_i) \cdot (\mathbf{J}_1 - \psi_i^* \mathbf{J}_2)^{\mathrm{H}} (\mathbf{q}_i \mathbf{U}_{s1}^{\dagger})^{\mathrm{H}} \\ &= \mathbf{W}_i \left(\sum_{j=1}^{P} |x_{ij}|^2 \mathrm{Var}(\delta\mathbf{u}_j) \right) \mathbf{W}_i^{\mathrm{H}} \end{aligned} \tag{B.19}$$

where $\mathbf{W}_i = \mathbf{q}_i \mathbf{U}_{s1}^{\dagger}(\mathbf{J}_1 - \psi_i^* \mathbf{J}_2)$.

It is shown in [14] that the errors between the eigenvectors of a Hermitian matrix have the following properties:

$$\mathrm{Var}(\delta\mathbf{u}_j) = \frac{\lambda_j}{N} \sum_{\substack{k=1 \\ k \neq j}}^{M} \frac{\lambda_k}{(\lambda_j - \lambda_k)^2} \mathbf{u}_k \mathbf{u}_k^{\mathrm{H}}, \quad j = 1, \ldots, M \tag{B.20}$$

where $\delta\mathbf{u}_i \triangleq \hat{u}_i - \mathbf{u}_i$ is the eigenvector error of $\mathbf{u}_i$. In the NCE covariance matrix, since $\lambda_{K+1} = \cdots = \lambda_M = 0$, (B.20) is reduced to be

$$\mathrm{Var}(\delta\mathbf{u}_j) = \frac{\lambda_j}{N} \sum_{\substack{k=1 \\ k \neq j}}^{K} \frac{\lambda_k}{(\lambda_j - \lambda_k)^2} \mathbf{u}_k \mathbf{u}_k^{\mathrm{H}}, \quad j = 1, \ldots, K \tag{B.21}$$

Therefore, substituting (B.21) into (B.19) yields

$$\mathrm{Var}(\breve{\delta\psi}_i) = \mathbf{W}_i \left(\sum_{j=1}^{P} \left| x_{ij} \right|^2 \frac{\lambda_j}{N} \sum_{\substack{k=1 \\ k \neq j}}^{K} \frac{\lambda_k}{(\lambda_j - \lambda_k)^2} \mathbf{u}_k \mathbf{u}_k^{\mathrm{H}} \right) \mathbf{W}_i^{\mathrm{H}}. \tag{B.22}$$

Substituting (B.22) into (B.7) completes the derivation of the MSE for the proposed method.

References

[1] R.O. Schmidt, Multiple emitter location and signal parameter estimation, IEEE Transactions on Antennas and Propagations 34 (3) (1986) 276–280.

[2] R.H. Roy, T. Kailath, ESPRIT-estimation of parameters via rotational invariance techniques, IEEE Transactions on Acoustics, Speech, and Signal Processing 37 (7) (1989) 984–995.

[3] S. Marcos, A. Marsal, M. Benidir, The propagator method for source bearing estimation, Signal Processing 42 (2) (1995) 121–138.

[4] J. Xin, A. Sano, Computationally efficient subspace-based method for direction-of-arrival estimation without eigendecomposition, IEEE Transactions on Signal Processing 52 (4) (2004) 876–893.

[5] A. Nicholas, J.W. Patrick, Estimating principal components of large covariance matrices using the Nyström method, in: IEEE International Conference on Acoustics, Speech, and Signal Processing (ICASSP), Prague, Czech Republic, 2011, pp. 3784–3787.

[6] P. Drineas, W.M. Micheal, On the Nyström method for approximating a Gram matrix for improved kernel-based learning, Journal of Machine Learning Research 6 (2005) 2153–2175.

[7] C.K.I. Williams, M. Seeger, Using the Nyström method to speed up kernel machines, in: Advances in Neural Information Processing Systems 2000, MIT Press, 2001.

[8] C. Fowlkes, Spectral grouping using the Nyström method, IEEE Transactions on Pattern Analysis and Machine Intelligence 26 (2) (2004) 214–225.

[9] J. Shi, J. Malik, Normalized cuts and image segmentation, IEEE Transactions on Pattern Analysis and Machine Intelligence 22 (8) (2000) 888–905.

[10] C. Qian, L. Huang, A low-complexity Nyström-based algorithm for array subspace estimation, in: 2012 Second International Conference

on Instrumentation, Measurement, Computer, Communication and Control (IMCCC), Harbin, China, 2012, pp. 112–114.
[11] B.D. Rao, K.V.S. Hari, Performance analysis of ESPRIT and TAM in determining the direction-of-arrival of plane waves in noise, IEEE Transactions on Acoustics, Speech, and Signal Processing 37 (12) (1989) 1990–1995.
[12] F. Li, H. Liu, R.J. Vaccaro, Performance analysis for DOA estimation algorithms: unification, IEEE Transactions on Aerospace and Electronic Systems 29 (1993) 1170–1184.
[13] F. Li, R.J. Vaccaro, D.W. Tufts, Performance analysis of the state-space realization (TAM) and ESPRIT algorithms for DOA estimation, IEEE Transactions on Antennas and Propagations 39 (1991) 418–423.
[14] D.R. Brillinger, Time Series: Data Analysis and Theory, Holt, Rhinehart and Winston, New York, 1975.
[15] R.E. Skelton, D.A. Wagie, Minimal root sensitivity in linear systems, Journal of Guidance (1984) 570–574.